

Thermoanalytical and Solution Stability Studies of Hexamethylenedithiocarbamates

Valéria D. Benedini,^a Patrícia A. Antunes,^b Éder T. G. Cavalheiro^{*,a} and Gilberto O. Chierice^a

^aInstituto de Química de São Carlos, Universidade de São Paulo, CP 780, 13560-970 São Carlos-SP, Brazil

^bUniversidade do Oeste Paulista, Rua José Bongiovani, 700, 19050-680 Presidente Prudente-SP, Brazil

Estudos termogravimétricos e calorimétricos exploratórios diferenciais de hexametileno-ditiocarbamatos de níquel(II), cobre(II), zinco(II) e cádmio(II) foram realizados sob atmosferas dinâmicas de ar e nitrogênio, para avaliar as etapas e os produtos de decomposição térmica. Esses produtos, quando cristalinos, foram caracterizados por difratometria de raios X, sendo predominantemente constituídos por sulfetos e óxidos metálicos sob N₂ e ar, respectivamente. Usando espectrofotometria na região do ultravioleta, também foram determinados o pK_a = 3,6 ± 0,2 para o ácido hexametilenoditiocarbâmico em força iônica igual a 0,50 mol dm⁻³ (KCl) a 25,0 °C e os parâmetros cinéticos de decomposição em diferentes valores de pH (k_{lim} = 2,21 × 10⁻² s⁻¹ e t_{1/2 lim} = 156 s).

Thermogravimetric and differential scanning calorimetric investigation of the thermal behavior of nickel(II), copper(II), zinc(II) and cadmium(II) hexamethylenedithiocarbamates were performed under nitrogen and air atmospheres in order to investigate the steps and products of thermal decomposition. When obtained in a crystalline form, the decomposition products were identified by their X-ray diffraction patterns. Metal sulfides and oxides were the major residues under nitrogen and air atmospheres, respectively. Spectrophotometric measurements in the ultraviolet region were used to estimate the pK_a = 3.6 ± 0.2 for the hexamethylenedithiocarbamic acid at 0.50 mol dm⁻³ ionic strength (KCl) at 25.0 °C and the kinetic parameters of decomposition at different pH values (k_{lim} = 2.21 × 10⁻² s⁻¹ and t_{1/2 lim} = 156 s).

Keywords: hexamethylenedithiocarbamate, thermogravimetry, differential scanning calorimetry, decomposition rate constant

Introduction

Dithiocarbamates (DTC) are products of the reaction between a primary or secondary amine and carbon disulfide in basic media. Their versatility and applicability was discussed by Kitson.¹ The interest in the solution stability of dithiocarbamates has been renewed by the utilization of such compounds as coadjutants in the treatment of AIDS,^{2,3} but they have also been suggested for tuberculosis⁴ and cancer⁵ treatment in the past. These applications demand enough chemical stability for an effective action in the biological medium.

The applications of this class of compounds are not limited to medicine and their use in agriculture, industry, analytical and organic chemistry, as well as their physicochemical properties, are summarized in several

review articles.⁶⁻¹⁵ From these works it is known that dithiocarbamates obtained from cyclic amines are more stable than the aliphatic derivatives.

The stability of dithiocarbamates in solution is strongly dependent on the pH, as discussed by several authors.¹⁶⁻²² However, it was the work of Chakrabarti and co-workers¹⁹⁻²² that led to the proposition of a decomposition intermediate whose stability is related to the presence of a water molecule in its structure.

Considering that the decomposition of dithiocarbamates is very fast in acidic media, a spectrophotometric method based on diode-array measurements has been proposed²³ in order to reach a more accurate determination of the pK_a of dithiocarbamic acids. A correlation between the infrared spectroscopy data of the coordination nature of cyclic DTC complexes and its effect on the thermal decomposition of such compounds has also been presented.^{24,25}

Hexamethylenedithiocarbamate (hex) is a cyclic DTC derived from hexamethyleneimine (homopiperidine), a

*e-mail: cavalheiro@iqsc.usp.br

seven member heterocyclic amine, whose structure is represented in Figure 1.

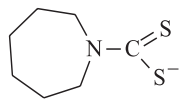


Figure 1. Structure of the hexamethylenedithiocarbamate.

Among many other applications, hex complexes have widely been used in the determination of several metals using different strategies and techniques for pre-concentration. Examples of such applications, presented during the last 35 years, include the recent description of the profitable use of $\text{Co}(\text{hex})_3$,²⁶⁻³³ $\text{Fe}(\text{hex})_3$,³³⁻³⁷ and its mixtures with $\text{Fe}_2\text{O}_3 \cdot x\text{H}_2\text{O}$ ³⁸⁻⁴² and $\text{Pb}(\text{hex})_2$ ⁴³⁻⁴⁶ as a colloidal precipitate collector in the flotation pre-concentration of Cd, Cu, Fe, Ni, Pb, Zn, Tl, Cr and Mn, allowing determinations at the ng dm^{-3} range in several water samples.

These complexes have also been used to pre-concentrate metal ions in columns. After this step, the complexes are eluted and inserted in HPLC systems, allowing separations and simultaneous quantifications.⁴⁷⁻⁵² They have also been employed in separation and co-precipitation⁵³⁻⁶⁰ and in the less recent applications with solid⁶¹⁻⁶⁴ and liquid phase extractions⁶⁵⁻⁷⁵ followed by determination by atomic spectroscopic techniques of several elements.

Studies regarding the standard enthalpy of formation of hexamethyleneaminium hexamethylenedithiocarbamate,⁷⁶ dye-sensitized photolysis⁷⁷⁻⁷⁹ and crystal structures of ligand and complexes^{80,81} can also be found.

Thermal analysis of mixed-ligand nickel hexamethylenedithiocarbamate complexes with triphenyl and tributylphosphine,⁸² as well as of lanthanide complexes with hexamethylenedithiocarbamate,^{83,84} have been described. Recently, the thermal behavior of the ammonium and hexamethyleneaminium salts of hexamethylenedithiocarbamate was also reported.⁸⁵

The solution stability of the hexamethylenedithiocarbamate proved to be important in medical applications. A representative example is the patent presented by the French Roussel-Uclaf company⁸⁶ regarding the use of this DTC as a protector of hepatic cells. The compound is taken orally or by a bloodshot as an alkaline cation salt solution. In addition, the thermal behavior is another important feature in industrial and agricultural application of this dithiocarbamate, as related to thermal stability and residues generated during thermal decomposition.⁷

Despite the importance of the solution and thermal stability for hex applications, few studies regarding these issues have been reported. In the present work, the pK_a

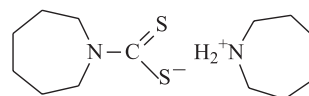
value of the hexamethylenedithiocarbamic acid (Hhex) was determined in ionic strength $I = 0.50 \text{ mol dm}^{-3}$ by spectrophotometry in the ultraviolet region, and used to estimate the decomposition rate of hexamethylenedithiocarbamate (hex) at different pH values using a method based on diode-array measurements of the absorbance.²³ Additionally, the thermal behavior of $\text{M}(\text{hex})_2$ ($\text{M} = \text{nickel(II), copper(II), zinc(II) and cadmium(II)}$) solid state complexes was evaluated, as these compounds are important examples of hex complexes with industrial and agricultural applications.

Experimental

All reagents were of analytical grade and used without further purification. The water employed in all experiments was deionized before use.

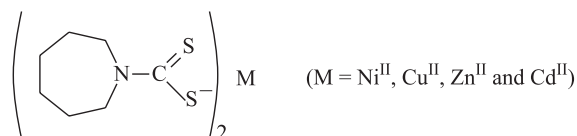
Hexamethyleneaminium-hexamethylenedithiocarbamate (HMA-hex) - synthesis and characterization

The HMA-hex salt was obtained by dissolving 0.4 mol of hexamethyleneimine in 50 dm^3 of ethanol/water 1:1 (v/v) in an erlenmeyer. The mixture was kept in an ice bath and protected from the light. Nitrogen was bubbled into the solution for 5 min and then 0.2 mol of carbon disulfide was slowly added to the reaction mixture. The white solid thus obtained was filtered, washed with cold ethanol and then dissolved in a minimum amount of ethanol/water 1:1 (v/v) at 35 °C, protected from the light. The solution was frozen and the white needle-like crystals were dried in a vacuum oven at 35 °C for 8 h and characterized as:



Hexamethylenedithiocarbamate complexes - synthesis and characterization

The metal complexes were obtained by direct reaction of the HMA-hex solution and $\text{CdCl}_2 \cdot 2\text{H}_2\text{O}$, $\text{CuCl}_2 \cdot \text{H}_2\text{O}$, $\text{NiCl}_2 \cdot 6\text{H}_2\text{O}$ and ZnCl_2 solutions in a glove bag (Cole-Parmer, USA) under N_2 . The resulting precipitates, with characteristic colors, were filtered off, washed with water and then with ethanol. They were finally dried in a vacuum oven at 35 °C for 8 h and characterized as:



Buffer solutions

The McIlvaine buffer solutions with ionic strength adjusted to 0.50 mol dm^{-3} (KCl) were prepared according to the procedure described by Elving *et al.*⁸⁷ The pH values of these buffers were accurately measured with a glass electrode previously calibrated with KCl solutions of ionic strength 0.50 mol dm^{-3} and hydrogen ion concentration 1.00×10^{-2} and $1.00 \times 10^{-4} \text{ mol dm}^{-3}$ (HClO_4), corresponding to pH 2.00 and 4.00, respectively.⁸⁸

Equipment

The characterization of the complexes was performed by IR vibrational spectroscopy (KBr pellets) in a Nicolet 5SXC spectrophotometer. Flame atomic absorption spectroscopy was carried out in a Hitachi Z-8100 spectrophotometer and C, N, H contents were determined by elemental analysis using a Fisons EA 1108 CNHS-O instrument.

Thermogravimetric (TG) curves were recorded in a DuPont 9900 thermoanalyser coupled with a TGA 951 Thermogravimetric Module, under a gas flow of $90 \text{ dm}^3 \text{ min}^{-1}$ (N_2 or air) in a platinum crucible. A heating rate of $10 \text{ }^\circ\text{C min}^{-1}$ and samples of about 7 mg at atmospheric pressure were employed. The differential scanning calorimetric (DSC) curves were recorded in a DuPont 9900 thermoanalyser coupled with a DSC 910 Calorimetric Module under a gas flow of $90 \text{ dm}^3 \text{ min}^{-1}$ (N_2 or air), in covered aluminum pans with a central pin hole, at a heating rate of $10 \text{ }^\circ\text{C min}^{-1}$ and using samples of about 5 mg at atmospheric pressure. The cell was previously calibrated for temperature and energy (ΔH) using indium metal (99.9+%) as standard.

Intermediates of the thermal decomposition process were generated in an oven at the same temperature and atmosphere in which they appeared in the TG curves. After 15 min of heating, they were cooled down and kept in a desiccator under vacuum. The X-ray patterns of the crystalline residues were recorded in a VEB-Karl Zeiss Jena URD6 diffractometer. The results were compared with standard data from the International Centre for Diffraction Data.⁸⁹

A diode-array Hewlett-Packard HP 8451A spectrophotometer and quartz cells, 1.00 cm path length, were used in the spectrophotometric measurements. The pH values were measured with a Corning IA 250 coupled to a Metrohm EA 121 combined glass electrode.

Procedure for pK_a determination

The spectrophotometric method used for pK_a determination was described earlier.^{23,90} All the spectrophotometric measurements were carried at $25.0 \pm 0.1 \text{ }^\circ\text{C}$, using the buffered solution as a blank. Stock HMA-hex solutions ($1.0 \times 10^{-2} \text{ mol dm}^{-3}$) were used in the preparation of working solutions, with concentrations ranging from 3.34×10^{-5} to $1.67 \times 10^{-6} \text{ mol dm}^{-3}$ in pH 2.13 and 8.40. A $1.0 \times 10^{-4} \text{ mol dm}^{-3}$ HMA-hex solution was used in the determination of the maximum absorption wavelength of the acidic and basic forms, in pH ranging from 2.78 to 4.10. In order to minimize the decomposition of the compounds, the solutions were prepared directly in the cells, by adding an appropriate volume of the stock solution of HMA-hex to the buffer solution and reaching a final volume of 3.00 dm^3 .

Results and Discussion

The products are listed in Table 1 and the formulae given are in agreement with elemental analyses and thermogravimetric data. The hex structure is presented in Figure 1. All complexes are anhydrous. The split IR absorption band around 1000 cm^{-1} indicated that the ligand presents a monodentate behavior in $\text{Cd}(\text{hex})_2$ and $\text{Zn}(\text{hex})_2$, while a single absorption band in this region suggests a bidentate behavior in $\text{Ni}(\text{hex})_2$ and $\text{Cu}(\text{hex})_2$, according to Sharma⁷ and Nakamoto.⁹¹ This is in total agreement with our previous findings for other cyclic DTC complexes with the same metal cations.^{24,25,90}

The characteristic C–N stretching vibrational mode is observed at $1474\text{--}1503 \text{ cm}^{-1}$ and is less intense than that observed for alkyl DTC derivatives due to the low double bond character caused by the rigid ring system.⁹²

Table 1. Percentages of metal, carbon, hydrogen and nitrogen found (calculated) and main infrared absorption bands (cm^{-1}) for the hexamethylenedithiocarbamates studied in this work

Compound(color)	Metal	C	H	N	$\nu(\text{C-N})$	$\nu(\text{C-S})$
HMA-hex(white)	-	56.8 (56.9)	9.89 (9.55)	9.75 (10.2)	1474	956,975
$\text{Ni}(\text{hex})_2$ (green)	13.3 (14.4)	40.2 (41.3)	5.84 (5.94)	6.56 (6.88)	1503	980
$\text{Cu}(\text{hex})_2$ (brown)	14.2 (15.4)	41.2 (40.8)	5.93 (5.87)	6.77 (6.80)	1500	985
$\text{Zn}(\text{hex})_2$ (white)	15.9 (15.8)	41.0 (40.6)	5.99 (5.84)	6.85 (6.77)	1485	959,982
$\text{Cd}(\text{hex})_2$ (white)	23.1 (24.4)	35.8 (36.5)	5.16 (5.25)	5.94 (6.08)	1485	959,979

pK_a determination

The use of diode array data for pK_a determination is convenient, since the decomposition of DTC is very fast in acidic media.¹⁹⁻²³ The decomposition rate depends on the amine substituents. The procedure considers that the total absorbance at a given wavelength is due to the sum of the absorbances of the protonated (Hhex) and free (hex) forms of the DTC:

$$A_A = \epsilon_{A,Hhex}[Hhex] + \epsilon_{A,hex}[hex] \quad (1)$$

$$A_B = \epsilon_{B,Hhex}[Hhex] + \epsilon_{B,hex}[hex] \quad (2)$$

in which A_A and A_B are the absorbances in the wavelengths A and B, respectively, $\epsilon_{A,Hhex}$ and $\epsilon_{A,hex}$ are the molar absorptivities of the protonated and free forms in the wavelength A, and [Hhex] and [hex] are the concentrations of the protonated and free forms, respectively. The absorptivity coefficients can be obtained from the slopes of A versus [hex] plots, at the maximum wavelengths, in acidic and basic media. On solving equations (1) and (2), it is possible to determine the [hex]/[Hhex] ratio. Then, measuring the absorbances at different pH values, the pK_a can be determined by the Henderson-Hasselbach equation:

$$pK_a = pH - \log \frac{[hex^-]}{[Hhex]} \quad (3)$$

The maximum absorption wavelength of the protonated (Hhex) form was observed at 276 nm. The free form presented two maxima at 260 and 283 nm. For best resolution, 260 nm (basic, $\epsilon = 1.22 \times 10^4 \text{ cm}^{-1} \text{ mol dm}^{-3}$) and 276 nm (acidic, $\epsilon = 1.06 \times 10^4 \text{ cm}^{-1} \text{ mol dm}^{-3}$) were used in the pK_a determination. The results are summarized in Table 2 and a pK_a value of 3.6 ± 0.2 was obtained. Values of pK_a around 3.29 were previously reported using a conventional spectrophotometric²¹ method at 25 °C and a 0.01 mol dm⁻³ ionic strength.

An evaluation of these differences can be performed considering the changes in spectral shape when the pH is changed from 2.8 to 4.1 (Figure 2). According to Vandebek *et al.*,²¹ the acidic form of a DTC presents

Table 2. Results of the pK_a determination for Hhex ($I = 0.50 \text{ mol dm}^{-3}$, 25 °C)

pH	absorbance		[hex]/[Hhex]	pK_a
	260 nm	276 nm		
2.78	0.445	0.713	0.246	3.41
3.39	0.551	0.696	0.854	3.47
4.21	0.735	0.741	3.59	3.65
4.79	0.819	0.778	7.35	3.93
			Mean \pm sd*	3.6 ± 0.2

*sd = standard deviation (n=4).

only one peak in the UV region, while the basic form presents two peaks. Figure 2 shows that from pH 3.9 two peaks are clearly observed, evidencing the presence of a significant amount of the basic form. At pH 2.8 only one peak is observed, suggesting the presence of a significant amount of the acidic form.

The results also suggest the following order of acidity for cyclic dithiocarbamate derivatives such as pyrrolidine (pyr), piperidine (pip), morpholine (mor) and hexamethylenedithiocarbamates (hex) (in brackets the pK_a value and the reference in which it appears):

Hpyr (3.14)²³ > Hpip (3.51)²³ \approx Hmor (3.56)⁹⁰ \approx Hhex (3.6)^{this work}

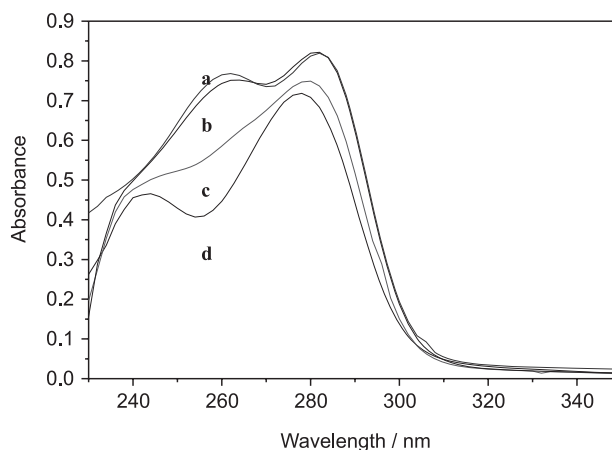


Figure 2. Changes in the UV-Vis spectral shape of a $1.0 \times 10^{-4} \text{ mol dm}^{-3}$ Hhex solution at different pH values: a) 4.1, b) 3.9, c) 3.6 and d) 2.8.

Decomposition kinetics

The decomposition of HMA-hex was followed by the absorbance decay of the 286 nm peak at different pH values. The $\ln A/A_0$ versus time plots showed a linear dependence, suggesting a pseudo-first order kinetics with slope equal to k_{ap} .

Chakrabarty and co-workers¹⁹⁻²² investigated the decomposition of dithiocarbamates. According to these authors, the rate of decomposition in basic media is dependent on the pH ($[H^+] \ll K_a$), but in sufficiently acidic solutions ($[H^+] \gg K_a$) it becomes constant ($k_{ap} \approx k_{lim}$), according to:

$$k_{ap} = k_{lim} \left(\frac{[H^+]}{[H^+] + K_a} \right) \quad (4)$$

in which k_{ap} is the apparent rate constant from the $\ln A/A_0$ versus time plots, k_{lim} is the limiting rate constant at low pH and K_a is the acidic dissociation constant.

The results obtained for hex are presented in Table 3. These data led us to conclude that hex presents an intermediate stability between the analogous

piperidinedithiocarbamate, pip ($t_{1/2\text{lim}} = 10$ s) and the 5 membered ring pyrrolidine derivative, pyr ($t_{1/2\text{lim}} = 1620$ s).²³ Chakrabati and co-workers^{20,21} attributed this difference to the ability of pyr and hex to interact with a water molecule in the decomposition intermediate, due to the configuration of the 5 and 7 membered rings.

The low stability of the anion in acidic medium can explain the large deviations between the measurements in Table 3.

Table 3. HMA-hex decomposition kinetic data at different pH values and at an ionic strength of 0.50 mol dm⁻³ (KCl)

pH	[H ⁺] / (10 ⁻³ mol dm ⁻³)	$k_{\text{ap}}/10^{-3} \text{ s}^{-1}$	$t_{1/2}/\text{s}$	$k_{\text{lim}}/(10^{-2} \text{ s}^{-1})$	$t_{1/2\text{lim}}/\text{s}$
2.10	7.94	62.87	11	6.48	10.7
2.75	1.78	1.98	350	0.225	308
3.98	0.105	0.770	900	0.257	270
4.92	0.0120	0.880	7880	1.88	36.8
			Mean	2.21	156

Thermal decomposition of solid state complexes

Thermal processes, residues formed, mass losses and temperature ranges observed in each step of the TG/DTG and DSC curves are given in Table 4 under nitrogen and Table 5 under air dynamic atmospheres. Crystalline intermediates were characterized by X-ray diffraction patterns and results were compared with literature data.⁸⁹ TG/DTG and DSC curves are presented in Figure 3 under

N₂ and in Figure 4 in air. DSC curves are limited to 600 °C because aluminum pans were used.

As described earlier,⁸⁵ the HMA-hex salt showed melting followed by complete volatilization between 110-163 and 90-170 °C under nitrogen and air dynamic atmospheres respectively (curves not presented). The IR spectra of the HMA-hex salt and of the condensed product confirmed the volatilization phenomena.

Crystalline changes were detected for the copper and the zinc complexes, represented by endothermic peaks in the DSC curves in both atmospheres. Melting points were checked by the use of a capillary tube immerse in a glycerin bath, in order to differentiate them from the crystalline changes. X-ray diffraction analysis was performed in order to characterize the crystalline residues, when available; otherwise the nature of the residues has been assigned by stoichiometric calculations. The results are presented in Table 6 and are compared with literature data.⁸⁹ The thermal behavior of the complexes is discussed below.

Thermal decomposition under nitrogen

Thermoanalytical curves are presented in Figure 3. According to TG/DTG and DSC data, there is no evidence for the presence of hydration water in the solids. Melting was observed for Cu(hex)₂, Cd(hex)₂, Ni(hex)₂ and Zn(hex)₂, and it was confirmed in a capillary glass tube

Table 4. Thermal degradation data under nitrogen, from thermogravimetry, showing the thermal process, the interval of temperature (ΔT), mass losses (Δm) experimental (exp) and calculated (calc), or residue and from differential scanning calorimetry, indicating the temperature of the peak (T), and the endothermic (endo) or exothermic (exo) nature of the process

Thermal Process (N ₂ Atmosphere)	$\Delta T / ^\circ\text{C}$ (TG)	$\Delta m^a / \%$		DSC Data T / °C
		Exp ^b	Calc.	
Cd(hex) ₂ (s) → Cd(hex) ₂ (l)	-	-	-	238.9 (endo)
Cd(hex) ₂ (l) → CdS ^c + CR ^d	222.8-416.5	39.7	-	312.6 (endo)
CdS + CR ^d → CdS	416.5-743.5	30.7	31.3	-
Cu(hex) ₂ (s ₁) → Cu(hex) ₂ (s ₂)	-	-	-	121.0 (endo)
Cu(hex) ₂ (s ₂) → Cu(hex) ₂ (l)	-	-	-	202.4 (endo)
Cu(hex) ₂ (l) → Cu(SCN) ₂	196.3-283.1	43.6	42.8	266.4 (endo)
Cu(SCN) ₂ → CuS ^c	283.1-605.6	23.2	23.8	407 (exo)
CuS → Cu ^o	605.6-864.4	15.4	16.9	-
Ni(hex) ₂ (s) → Ni(hex) ₂ (l)	-	-	-	268.0 (endo)
Ni(hex) ₂ (l) → 1/2Ni ₂ S ₃	275.0-400.6	26.2	26.2	334.5 (endo)
1/2Ni ₂ S ₃ → NiS	600.3-682.0	22.3	22.0	-
Zn(hex) ₂ (s ₁) → Zn(hex) ₂ (s ₂)	-	-	-	156.0 (endo)
Zn(hex) ₂ (s ₂) → Zn(hex) ₂ (l)	-	-	-	180.7 (endo)
Zn(hex) ₂ (l) → ZnS ^c	218.5-386.4	21.5	20.8	320.4 (endo)
ZnS → Zn ^o	432.0-735.0	16.0	14.4	-

^athe mass losses refer to the starting material; ^brelative to residue in relation to the starting material; ^ccharacterized by X-ray diffraction pattern – see Table 6; ^dCR = carbonaceous residue.

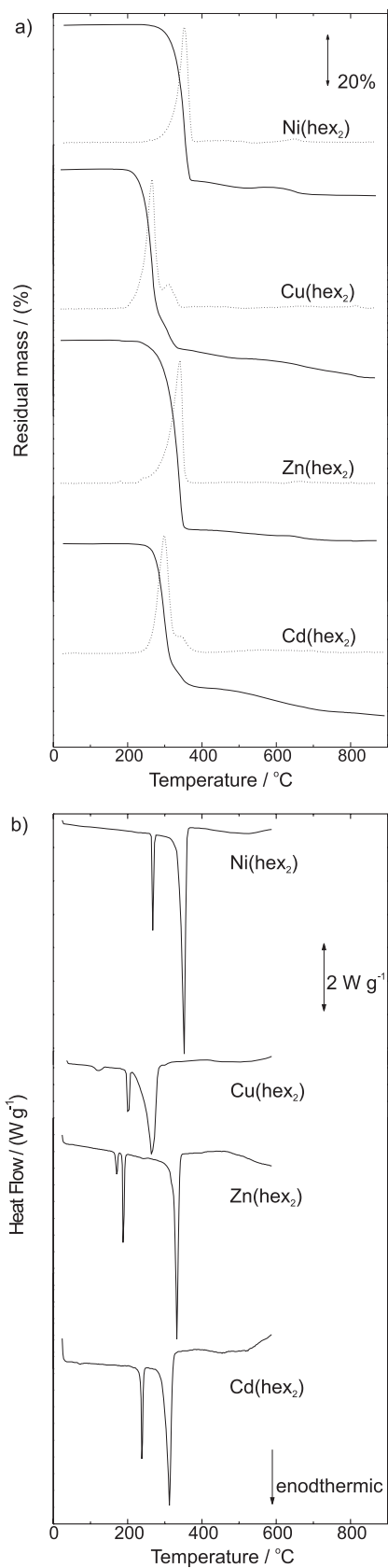


Figure 3. TG (solid)/DTG(dashed) (a) and DSC (b) curves under nitrogen flow of 90 dm³ min⁻¹, sample mass ca. 7mg, heating heat 10 °C min⁻¹, platinum sample holder (TG/DTG) and aluminum (DSC).

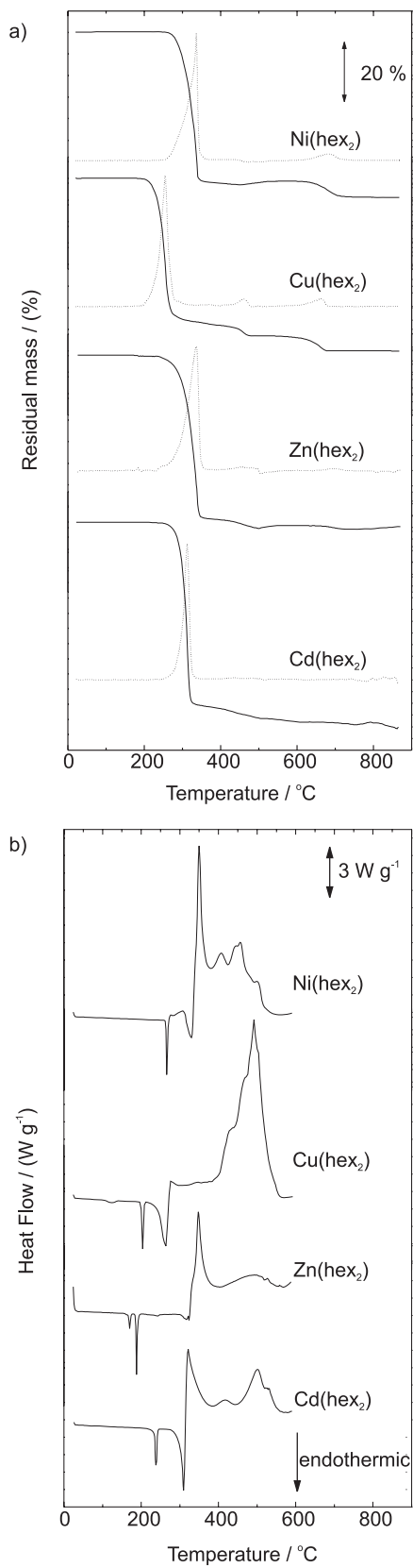


Figure 4. TG (solid)/DTG(dashed) (a) and DSC (b) curves under air flow of 90 dm³ min⁻¹, sample mass ca. 7mg, heating heat 10 °C min⁻¹, platinum sample holder (TG/DTG) and aluminum (DSC).

Table 5. Thermal degradation data under air, from thermogravimetry, showing the thermal process, the interval of temperature (ΔT), mass losses (Δm) experimental (exp) and calculated (calc), or residue and from differential scanning calorimetry, indicating the temperature of the peak (T), and the endothermic (endo) or exothermic (exo) nature of the process

Thermal Process (Air Atmosphere)	$\Delta T / ^\circ\text{C}$ (TG)	$\Delta m^a / \%$		DSC Data
		Exp. ^b	Calc.	T / $^\circ\text{C}$
$\text{Cd}(\text{hex})_2(\text{s}) \longrightarrow \text{Cd}(\text{hex})_2(\text{l})$	-	-	-	238.4 (endo)
$\text{Cd}(\text{hex})_2(\text{l}) \longrightarrow \text{CdS}^c$	227-617.8	31.3	31.2	309.6, 416.5 (endo) 321.7, 501.7 (exo)
$\text{CdS} \longrightarrow \frac{1}{2}\text{Cd}_2\text{OSO}_4$	680.0-794.6	34.0	36.5	
$\frac{1}{2}\text{Cd}_2\text{OSO}_4 \longrightarrow$ decomposition products	>800	-	-	-
$\text{Cu}(\text{hex})_2(\text{s1}) \longrightarrow \text{Cu}(\text{hex})_2(\text{s2})$	-	-	-	123.5 (endo)
$\text{Cu}(\text{hex})_2(\text{s2}) \longrightarrow \text{Cu}(\text{hex})_2(\text{l})$	-	-	-	204.0 (endo)
$\text{Cu}(\text{hex})_2(\text{l}) \longrightarrow \frac{1}{2}\text{Cu}_2\text{S}(\text{CN})_2^c$	187.2-387.9	32.0	-	264.5 (endo)
$\frac{1}{2}\text{Cu}_2\text{S}(\text{CN})_2 \longrightarrow \frac{1}{2}\text{Cu}_2\text{OSO}_4$	387.9-476.7	27.1	29.0	492.0 (exo)
$\frac{1}{2}\text{Cu}_2\text{OSO}_4 \longrightarrow \text{CuO}^b$	568.4-681.3	19.3	19.8	
$\text{Ni}(\text{hex})_2(\text{s}) \longrightarrow \text{Ni}(\text{hex})_2(\text{l})$	-	-	-	260.0 (endo)
$\text{Ni}(\text{hex})_2(\text{l}) \longrightarrow \frac{1}{2}\text{Ni}_2\text{S}_3$	244.4-430.5	26.2	28.3	308.0 (endo), 349.3 (exo)
$\frac{1}{2}\text{Ni}_2\text{S}_3 \longrightarrow \frac{1}{2}\text{Ni}_2\text{OSO}_4$	467.6-517.3	28.2	29.0	407.0, 456.3, 502.4 (exo)
$\frac{1}{2}\text{Ni}_2\text{OSO}_4 \longrightarrow \frac{1}{2}\text{Ni}_2\text{O}_3$	621.1-729.5	23.4	20.3	-
$\text{Zn}(\text{hex})_2(\text{s1}) \longrightarrow \text{Zn}(\text{hex})_2(\text{s2})$	-	-	-	162.4 (endo)
$\text{Zn}(\text{hex})_2(\text{s2}) \longrightarrow \text{Zn}(\text{hex})_2(\text{l})$	-	-	-	185.0 (endo)
$\text{Zn}(\text{hex})_2(\text{l}) \longrightarrow \text{ZnS}^c$	206.5-380.0	23.5	22.2	316.5 (endo), 348.0 (exo)
$\text{ZnS} \longrightarrow \text{ZnO}$	390.6-729.5	19.7	19.5	-

^athe mass losses refer to the starting material; ^brelative to residue in relation to the starting material; ^ccharacterized by X-ray diffraction pattern – see Table 6.

Table 6. X-ray diffraction data for the residues at different temperatures, compared with literature standards^a

Compound	residue at/standard	d / \AA							
$\text{Cd}(\text{hex})_2$	350 $^\circ\text{C}$ (N_2)	3.57	3.35	3.15	2.06	1.39	-	-	-
	CdS^a	3.58	3.36	3.16	2.07	1.39	-	-	-
	700 $^\circ\text{C}$ (N_2)	3.58	3.35	3.16	2.45	2.07	1.90	1.76	-
	CdS^a	3.58	3.35	3.16	2.45	2.07	1.90	1.76	-
$\text{Cu}(\text{hex})_2$	480 $^\circ\text{C}$ (N_2)	3.01	2.74	2.30	1.90	1.88	1.75	1.24	-
	CuS^a	3.04	2.72	2.31	1.90	1.89	1.74	1.23	-
	850 $^\circ\text{C}$ (N_2)	2.08	1.28	1.08	1.06	-	-	-	-
	Cu^a	2.08	1.28	1.09	1.04	-	-	-	-
	330 $^\circ\text{C}$ (air)	3.24	2.85	-	1.99	1.69	-	-	-
$\text{Zn}(\text{hex})_2$	$\text{Cu}_2\text{S}(\text{CN})_2^a$	3.18	2.88	2.30	1.97	1.70	-	-	-
	850 $^\circ\text{C}$ (air)	2.52	2.32	1.86	1.58	1.50	1.42	1.38	1.28
	CuO^a	2.54	2.34	1.87	1.59	1.51	1.42	1.38	1.27
$\text{Zn}(\text{hex})_2$	400 $^\circ\text{C}$ (N_2)	3.12	2.03	1.67	1.35	1.25	1.10	1.03	-
	ZnS^a	3.12	1.91	1.63	1.35	1.24	1.10	1.04	-

^adata from reference 89.

test. $\text{Zn}(\text{hex})_2$ and $\text{Cu}(\text{hex})_2$ apparently melted after a crystalline transition, as suggested by the peak shape and the absence of mass loss associated with the process. XRD measurements were not performed before and after the peak in order to confirm these physical changes.

Sulfides were the main residues around 400 $^\circ\text{C}$, after the decomposition of the complexes. Metallic Cd, Cu and Zn were found in the further decomposition steps of the inorganic residue, while NiS remained stable as the final decomposition product in the temperature range investigated.

Only in the $\text{Cu}(\text{hex})_2$ case, $\text{Cu}(\text{SCN})_2$ was detected as the intermediate in decomposition, as suggested by Sharma.⁷ This is in agreement with previous findings for other cyclic dithiocarbamate derivatives.^{23-25,90}

Thermal decomposition in air

The thermoanalytical curves recorded in air are presented in Figure 4. For Cd, Ni and Zn complexes, the respective sulfides were produced after the first

decomposition step and were converted to oxide (Zn) or oxysulfates (Cd and Ni) by further heating of the residue (see Table 5). The detection of oxysulfates as decomposition intermediates is in agreement with previous results.²⁴ The copper complex decomposed in a different way, generating $\text{Cu}_2\text{S}(\text{CN})_2$, oxysulfate and finally the oxide, according to the X-ray diffraction patterns of the residues.⁸⁹ Crystalline changes and melting processes were also observed, in agreement with the data obtained under N_2 and reported in the previous section.

Results indicated that the following stability order can be established, according to the temperature in which decomposition starts: $\text{Ni}(\text{hex})_2 > \text{Cd}(\text{hex})_2 > \text{Zn}(\text{hex})_2 > \text{Cu}(\text{hex})_2$.

Conclusions

The Hhex is the weaker acid when compared to the series of cyclic DTC derived from pyrrolidine, piperidine and hexamethyleneamine, respectively 5, 6 and 7-membered aminic rings. The limiting half life ($t_{1/2\text{lim}}$) suggests that hex is more stable than piperidinedithiocarbamate (pip) and morpholinedithiocarbamate (mor) and much less stable than pyrrolidinedithiocarbamate (pyr).^{23,90}

The thermal analytical studies revealed that sulfides were the main residues obtained under nitrogen atmosphere, which were reduced to the elementary metals in the case of the copper(II) and zinc(II) complexes. Oxysulfates were observed in air as intermediates of the decomposition of $\text{Ni}(\text{hex})_2$, $\text{Cu}(\text{hex})_2$ and $\text{Cd}(\text{hex})_2$, while oxides were obtained as final decomposition products. The nickel(II) complex was the most stable in this series.

References

1. Kitson, T.; *Education in Chemistry* **1985**, 43.
2. Rabbi, M.F.; Finnegan, A.; Al-Hartli, L.; Stong, S.; Roebuck K.A.; *Journal of Acquired Immune Deficiency Syndromes and Human Retrovirology* **1998**, 19, 321.
3. Topping, R.M.; Jones, M.M.; *Med. Hypothesis* **1989**, 27, 55.
4. Weuffen, A.; Kewitsch, A.; *Arch. Exp. Veterinaarmed.* **1967**, 21, 1049.
5. Powell, A.K.; *Brit. J. Cancer* **1954**, 8, 529.
6. Hill, J. O.; Chirawongaram, S.; *J. Thermal Anal.* **1994**, 41, 511.
7. Sharma, A.K.; *Thermochim. Acta* **1986**, 104, 339.
8. Magee, R.J.; Hill, J.O.; *Rev. Anal. Chem.* **1985**, 8, 5.
9. Bond, A.M.; Martin, R.L.; *Coord. Chem. Rev.* **1984**, 54, 23.
10. Sengupta, S.K.; Kumar, S.; *Thermochim. Acta* **1984**, 72, 349.
11. Hill, J.O.; Magee, R.J.; *Rev. Inorg. Chem.* **1981**, 3, 141.
12. Coucovanis, D.; *Progr. Inorg. Chem.* **1979**, 26, 301.
13. Coucovanis, D.; *Progr. Inorg. Chem.* **1970**, 11, 233.
14. Hulanicki, A.; *Talanta* **1967**, 14, 1371.
15. Thorn, G.D.; Ludwig, R.A.; *The Dithiocarbamates and Related Compounds*, Elsevier: Amsterdam, 1962.
16. Castro, E.A.; Cortes, R.; Santos, J.G.; Vega, J.C.; *J. Org. Chem.* **1982**, 47, 3774.
17. De-Filippo, D.; Deplano, P.; Devillanova, F.; Trogu, E.F.; Verani G.; *J. Org. Chem.* **1973**, 38, 560.
18. Usatenko, Y.I.; Barkalov, U.S.; Tulypa, F.M.; *J. Anal. Chem.-USSR* **1970**, 25, 1458.
19. Aspila, K.I.; Chakrabarti, C.L.; Sastri, V.S.; *Anal. Chem.* **1973**, 45, 363.
20. Joris, S.J.; Aspila, K.I.; Chakrabarti, C.L.; *J. Phys. Chem.* **1970**, 74, 860.
21. Vandebeek, R.R.; Joris, S.J.; Aspila, K.I.; Chakrabarti, C.L.; *Can. J. Chem.* **1970**, 48, 2204.
22. Aspila, K.I.; Sastri, V.S.; Chakrabarti, C.L.; *Talanta* **1969**, 16, 1099.
23. Cavalheiro, E.T.G.; Chierice, G.O.; *J. Braz. Chem. Soc.* **1997**, 8, 53.
24. Cavalheiro, E.T.G.; Ionashiro, M.; Marino, G.; Breviglieri, S.T.; Chierice, G.O.; *J. Braz. Chem. Soc.* **1999**, 10, 65.
25. Cavalheiro, E.T.G.; Ionashiro, M.; Marino, G.; Breviglieri, S.T.; Chierice, G.O.; *Transit. Metal Chem.* **2000**, 25, 69.
26. Bundalevska, J.M.; Koyuncu, I.; Ay, O.; Cundeva; K.; Akcin, G.; Stafilov, T.; *J. Environ. Sci. Health, Part A: Toxic/Hazard. Subst. Environ. Eng.* **2005**, 40, 1045.
27. Kojuncu, Y.; Bundalevska, J.M.; Ay, U.; Cundeva; K.; Stafilov, T.; Akcin, G.; *Sep. Sci. Technol.* **2004**, 39, 2751.
28. Ay, U.; Cundeva; K.; Stafilov, T.; Zajkova, V.P.; Pavlovskaa, G.; *Anal. Lett.* **2004**, 37, 695.
29. Cundeva; K.; Stafilov, T.; Pavlovskaa, G.; Karadjova, I.; Arpadjan, S.; *Int. J. Environ. Anal. Chem.* **2003**, 83, 1009.
30. Pavlovskaa, G.; Cundeva; K.; Stafilov, T.; Zendelovska, D.; *Sep. Sci. Technol.* **2003**, 38, 1111.
31. Pavlovskaa, G.; Cundeva; K.; Stafilov, T.; *Anal. Lett.* **2002**, 35, 2347.
32. Pavlovskaa, G.; Stafilov, T.; Cundeva; K.; *Fresenius. J. Anal. Chem.* **2001**, 369, 670.
33. Stafilov, T.; Cundeva; K.; Pavlovskaa, G.; *Int. J. Environ. Anal. Chem.* **2001**, 80, 269.
34. Stafilov, T.; Pavlovskaa, G.; Cundeva; K.; Zendelovska, D.; Paneva, V.; *J. Environ. Sci. Health, Part A: Toxic/Hazard. Subst. Environ. Eng.* **2001**, 360, 735.
35. Zendelovska, D.; Pavlovskaa, G.; Cundeva; K.; Stafilov, T.; *Talanta* **2001**, 54, 139.
36. Zendelovska, D.; Cundeva; K.; Stafilov, T.; *Mikrochim. Acta* **2000**, 135, 55.
37. Cundeva; K.; Stafilov, T.; Pavlovskaa, G.; *Microchem. J.* **2000**, 65, 165.
38. Stafilov, T.; Zendelovska, D.; Pavlovskaa, G.; Cundeva; K.; *Spectrochim. Acta, Part B* **2002**, 57, 907.

39. Pavlovska, G.; Cundeva, K.; Stafilov, T.; *Croatia Chemica Acta* **2001**, *74*, 121.
40. Stafilov, T.; Pavlovska, G.; Cundeva, K.; *Turk. J. Chem.* **2000**, *24*, 303.
41. Stafilov, T.; Pavlovska, G.; Cundeva, K.; *Microchem. J.* **1998**, *60*, 32.
42. Pavlovska, G.; Stafilov, T.; Cundeva, K.; *Fresenius. J. Anal. Chem.* **1998**, *361*, 213.
43. Paneva, V.Z.; Cundeva, K.; Stafilov, T.; *Spectrochim. Acta, Part B* **2005**, *60*, 403.
44. Cundeva, K.; Pavlovska, G.; Stafilov, T.; *J. Serb. Chem. Soc.* **2001**, *66*, 709.
45. Pavlovska, G.; Cundeva, K.; Stafilov, T.; *Sep. Sci. Technol.* **2000**, *35*, 2663.
46. Cundeva, K.; Stafilov, T.; Pavlovska, G.; *Spectrochim. Acta, Part B* **2000**, *55*, 1081.
47. Ichinoki, S.; Okamoto, Y.; Ishikuma, H.; Fujii, Y.; *J. Liq. Chromatogr. Relat. Technol.* **2003**, *26*, 2797.
48. Shijo, Y.; Yoshida, H.; Kitamura, T.; Yoshimoto, E.; Uehara, N.; *Anal. Sci.* **1996**, *12*, 761.
49. Ichinoki, S.; Yamazaki, M.; Omura, M.; Nagai, R.; *Bunseki Kagaku* **1996**, *45*, 837.
50. Falter, R.; Scholer, H.F.; *Fresenius J. Anal. Chem.* **1995**, *353*, 34.
51. Ichinoki, S.; Yamazaki, M.; *J. Chromatogr. Sci.* **1991**, *29*, 184.
52. Ichinoki, S.; Yamazaki, M.; *Anal. Chem.* **1985**, *57*, 662.
53. Frigge, C.; Jackwerth, E.; *Anal. Chim. Acta* **1993**, *271*, 299.
54. Buhler, A.; Jackwerth, E.; *Fresenius J. Anal. Chem.* **1992**, *343*, 362.
55. Fang, Z.L.; Dong, L.P.; *J. Anal. At. Spectrom.* **1992**, *7*, 439.
56. Fang, Z.L.; Sperling, M.; Welz, B.; *J. Anal. At. Spectrom.* **1991**, *6*, 301.
57. Frigge, C.; Jackwerth, E.; *Anal. Chim. Acta* **1991**, *242*, 99.
58. Byrko, V.M.; Vizhenskii, V.A.; Molchanova, T.P.; *J. Anal. Chem. USSR* **1987**, *42*, 251.
59. Yamamoto, Y.; Nishino, Y.; Ueda, K.; *Talanta* **1985**, *32*, 662.
60. Yamamoto, Y.; Sugita, M.; Ueda, K.; *Bull. Chem. Soc. Jpn.* **1982**, *55*, 742.
61. Tokahoglu, S.; Kartal, S.; Elci L.; *Bull Kor. Chem. Soc.* **2002**, *23*, 693.
62. Alexandrova, A.; Arpadjan, S.; *Anal. Chim. Acta* **1995**, *307*, 71.
63. Alexandrova, A.; Arpadjan, S.; *Analyst* **1993**, *118*, 1309.
64. Wommel, S.; Calmano, W.; *Acta Hydrochimica et Hydrobiologica* **1992**, 265.
65. Dapaah, A.R.K.; Takano, N.; Ayame, A.; *Anal. Chim. Acta* **1999**, *386*, 281.
66. Dapaah, A.R.K.; Ayame, A.; *Anal. Chim. Acta* **1998**, *360*, 26.
67. Dapaah, A.R.K.; Ayame, A.; *Anal. Sci.* **1997**, *13*, 405.
68. Miyazake, A.; Sampei, T.; Tao, H.; Nagase, T.; *Nippon Kagaku Kaishi* **1992**, 307.
69. Tao, H.; Miyazake, A.; Bamsho, K.; Unezaki, Y.; *Anal. Chim. Acta* **1984**, *156*, 159.
70. Tsalev, D.L.; Petrova, V.P.; *Dokladi Na Bolgarskata Akademiya Na Naukite* **1979**, *32*, 911.
71. Dornemann, A.; Kleist, H.; *Analyst* **1979**, *104*, 1030.
72. Tsalev, D.L.; *Dokladi Na Bolgarskata Akademiya Na Naukite* **1979**, *32*, 779.
73. Berndt, H.; Jackwerth, E.; *Fresenius J. Anal. Chem.* **1978**, *290*, 369.
74. Busev, A.I.; Tereshchenko, A.P.; Naidina, V.P.; *J. Anal. Chem. USSR* **1976**, *31*, 944.
75. Busev, A.I.; Byrko, V.N.; Tereshchenko, A.P.; Novikova, N.N.; Naidina, V.P.; Terentev, P.B.; *Zhurnal Analiticheskoi Khimii* **1970**, *25*, 665.
76. Alekseev, T.A.; Tresvyat, P.A.; Treshch, A.P.; *Russ. J. Phys. Chem.* **1971**, *45*, 1669.
77. Yamase, T.; Kokado, H.; Inoue, E.; *Bull. Chem. Soc. Jpn.* **1972**, *45*, 726.
78. Yamase, T.; Kokado, H.; Inoue, E.; *Bull. Chem. Soc. Jpn.* **1970**, *43*, 669.
79. Yamase, T.; Kokado, H.; Inoue, E.; *Bull. Chem. Soc. Jpn.* **1970**, *43*, 934.
80. Zvonkova, Z.V.; Yakovenk, V.I.; *Soviet Physics Crystallography* **1968**, *13*, 134.
81. Zvonkova, Z.V.; Poveteva, Z.P.; Vozzenni, V.M.; Gluskova, V.P.; Jakovenk, V.I.; Khvatkin, A.N.; *Acta Crystallographica S* **1966**, *21*, A155 Part 7S.
82. Pavlicek, M.; Travnicek, Z.; Pastorek, R.; Marek, J.; *Transition Met. Chem. (Dordrecht, Neth.)* **2003**, *28*, 260.
83. Dahiya, K.K.; Kaushik, N.K.; *Thermochim. Acta* **1989**, *141*, 69.
84. Dahiya, K.K.; Kaushik, N.K.; *Indian J. Chem., Sect. A: Inorg., Bio-inorg., Phys., Theor. Anal. Chem.* **1988**, *27*, 449.
85. Ramos, L.A.; Cavalheiro, E.T.G.; Chierice, G.O.; *J. Therm. Anal. Calorim.* **2005**, *79*, 349.
86. Roussel-Uclaf (ROUS); FR2081589-A5; FR2081589-A, 1970 (AN 1972: 501408).
87. Elving, P.J.; Morkowitz, J.M.; Rosenthal, I.; *Anal. Chem.* **1956**, *28*, 1179.
88. Cavalheiro, E.T.G.; Plepis, A.M.G.; Chierice, G.O.; Neves, E.F.A.; *Polyhedron* **1987**, *9*, 1717.
89. International Centre for Diffraction Data. Power Diffraction File (CD-ROM). Newton Square, ICDD, 1994.
90. Antunes, P.A.; Breviglieri, S.T.; Chierice, G.O.; Cavalheiro, E.T.G.; *J. Braz. Chem. Soc.* **2001**, *12*, 473.
91. Nakamoto, K.; *Infrared and Raman Spectra of Inorganic and Coordination Compounds*, 3rd ed.; John Wiley: New York, 1977.
92. Preti, C.; Tosi, G.; Zanini, P.; *J. Mol. Struct.* **1979**, *53*, 35.

Received: September 19, 2005

Published on the web: May 16, 2006

FAPESP helped in meeting the publication costs of this article.